

## Parametric Interaction of Modulated Intense Relativistic Electron Beams with High-Voltage Gaps

M. Friedman and V. Serlin

*Plasma Physics Division, Naval Research Laboratory, Washington, D.C. 20375*

(Received 29 January 1985)

A parametric mechanism that can tailor the shape of a modulated intense relativistic electron beam was found. This mechanism is highly efficient in up-conversion of the fundamental frequency of the current modulation to the second and third harmonics. It is shown in this Letter that the parametric mechanism is the result of a nonlinear capacitance that appeared when a quasi-dc high-density electron beam traversed a high-voltage gap.

PACS numbers: 52.75.-d, 41.80.-y

Parametric mechanisms have been used for many years in low-noise rf amplifiers,<sup>1</sup> in generation of shock waves in nonlinear electric lines,<sup>2</sup> and in explanation of free-electron laser mechanisms.<sup>3</sup> They also appeared in various plasma devices.<sup>4</sup> Parametric mechanisms originate in electrical circuits when some elements such as capacitors, inductors, dielectric constant, or wave velocity can be varied in time by applying a suitable signal. Examples of nonlinear elements are semiconductor diodes<sup>5</sup> (Varactors), ferrites,<sup>6</sup> and electron beams.<sup>7</sup>

In this Letter we investigate a parametric mechanism that originates from a nonlinear capacitance that appears in a high-voltage gap during the passage of a high-density electron beam. We find that when a high-density electron beam that is current modulated at a frequency  $f$  traverses a gap, high-voltage pulses at frequencies of  $2f$  and  $3f$  will appear in the gap influencing the current of the electron beam. The total effect is a highly efficient mechanism for up-conversion of the frequency of a density-modulated intense relativistic electron beam.

It is clear that the propagation of a dense electron beam within a geometry that includes high-voltage electrodes can affect the charge distribution, and hence the capacitance between the electrodes. In 1957 Bull suggested<sup>8</sup> that the dc capacitance of a parallel-plate capacitor depended on the current of the electron beam that flows through it and on the applied voltage. This effect was calculated and found to be of importance at high electron densities which corresponded to the space-charge-limited current. Since in 1957 high-current electron beams did not exist, the effect was never verified experimentally.

In the 1970's it became possible to generate high-density electron beams, the so-called intense relativistic electron beams (IREB's).<sup>9</sup> It also became possible recently to modify the spatial and temporal distribution of IREB's by propagation through high-voltage gaps.<sup>10-12</sup> The new experimental results suggest that the work of Bull should be revisited.

The capacitance per unit area of a one-dimensional

capacitor that consists of two parallel plates through which an electron beam of current  $I$  is propagating<sup>13</sup> is

$$C' = \frac{\partial}{\partial V_0} \left( \epsilon \frac{mc}{e} \frac{\beta_f \gamma_f - \beta_i \gamma_i}{T} + \delta \right) \quad (1)$$

where  $V_0$  is the applied voltage on the capacitor, the subscripts  $i$  and  $f$  stand for input and output, respectively,  $\gamma = (1 - \beta^2)^{-1/2}$ ,  $\beta = v/c$ , and  $v$  is the electron velocity.  $T$  is the transit time of electrons across the space between the two parallel plates,  $\delta = (Q_{Af} + Q/2)/A_0$  where  $Q$  is the total charge inside the capacitor,  $Q_{Af}$  is the image charge on the output plate, and  $A_0$  is the area of the plate.

For a low-density nonrelativistic electron beam  $\gamma_f \approx \gamma_i \approx 1$ ,  $Q/2 = -Q_{Af}$ ,  $\delta \approx 0$ , and  $T = d(\beta_f - \beta_i) \times mc/eV_0$  where  $d$  is the distance between the two parallel plates. In that case

$$C' = \epsilon/d. \quad (2)$$

This is the free-space capacitance per unit area of a two-parallel-plates capacitor.

When superrelativistic electrons traverse the capacitor the capacitance can be calculated taking  $\beta_f \approx \beta_i \approx 1$ ,  $\gamma_f = \gamma_i + eV_0/mc$ ,  $T = d/c$ , and  $Q/2 = -Q_{Af}$  or  $\delta \approx 0$ . In that case too,  $C' \approx \epsilon/d$ . Only for a high-density and mildly relativistic electron beam does  $C' \neq \epsilon/d$ . Moreover, it was shown<sup>13</sup> that for  $V_0 < 0$  the capacitance is  $C' > \epsilon/d$  and when  $V_0 > 0$  the capacitance is  $C' \leq \epsilon/d$ . Thus, the gap capacitance appears to be nonlinear, i.e.,  $C'$  depends on  $V_0$ .

A quantitative picture of the behavior of a realistic, two-dimensional gap can be found by investigation of the change of the potential energy stored in the gap as a function of  $V_0$ . The potential energy stored in a capacitor (of any shape) that is confined by two electrodes between which electrons with charge density  $\rho$  are stored is

$$W_k = \frac{1}{2} \epsilon \int E^2 d^3 l = \frac{1}{2} Q_f^* V_0 + \frac{1}{2} \epsilon \int \rho V d^3 l. \quad (3)$$

For simplicity it is assumed that one of the electrodes is grounded while the second one is held at a potential

Work of the U. S. Government

Not subject to U. S. copyright

$V_0$  and has a charge of  $Q_f^*$ . The symbol  $d^3l$  in Eq. (3) denotes volume integration and  $V$  is the potential at any point. Equation (3) can be written<sup>13</sup> as

$$W_k = \frac{1}{2} CV_0^2 + K \tag{4}$$

where  $C$  and  $K$  are constant when the current density flowing through the capacitor is small. Only when space-charge field becomes large will  $W_k$  deviate from the quadratic form.

To evaluate  $W_k$ , Poisson's equation

$$\Delta V = -\rho/\epsilon \tag{5}$$

was solved, with the assumption of  $\rho v = \text{constant}$ .  $V$  was the voltage calculated throughout the volume of the capacitor. Figure 1 shows an example of this calculation,

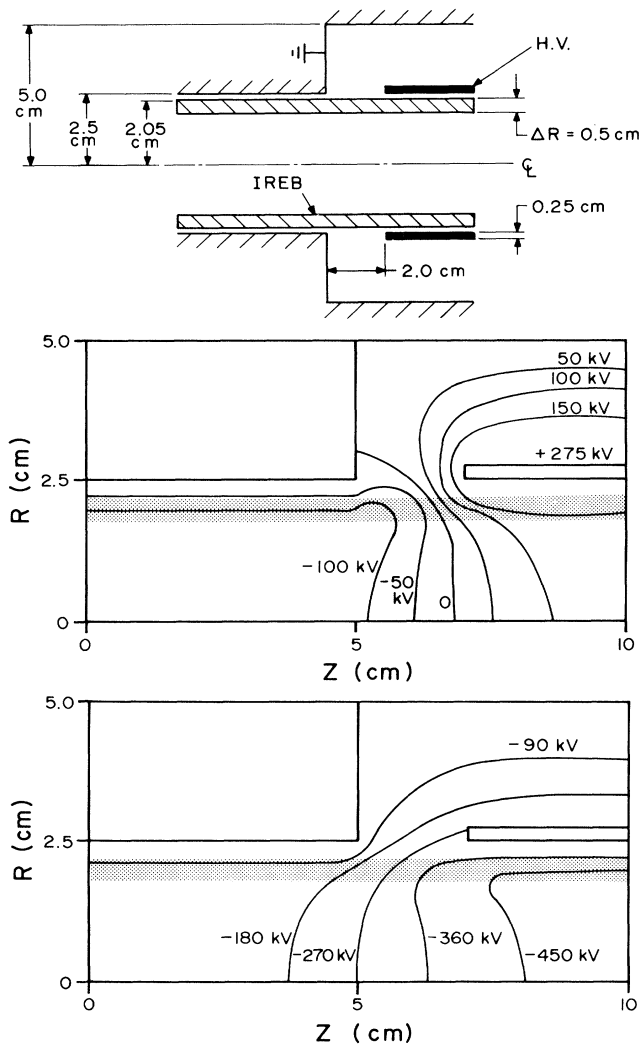


FIG. 1. (Top) The geometry of a two-dimensional gap. (Middle) Equipotential lines for the geometry at the top and for  $V_0 = +275$  kV. (Bottom) Equipotential lines for the geometry at the top and for  $V_0 = -275$  kV. The electron current was 8 kA and electron energy was 550 keV.

the equipotential lines for a realistic two-dimensional gap. The gap was inserted in a circular drift tube and the voltage was fed by a coaxial line. The geometrical parameters of the gap are shown in Fig. 1. The voltage on the gap was  $V_0 = +275$  kV and  $V_0 = -275$  kV. The electron beam, that was annular in shape, of 550-keV energy and with a current of 8 kA, propagated in the drift tube.

With use of this calculation it was possible to evaluate  $W_k$  vs  $V_0$  (Fig. 2). In this figure one sees that a critical current exists for which  $W_k$  is no longer quadratic with  $V_0$ .  $W_k$  is the potential energy that is "stored" and can be "retrieved" from the system by changing  $V_0$ . Hence, it can be associated with a capacitor of a value

$$C_g = V_0^{-1} \partial W_k / \partial V_0. \tag{6}$$

When  $W_k$  deviates from the quadratic form [Eq. (4)]  $C_g$  will become nonlinear (or voltage dependent).

As was mentioned earlier, a nonlinear electrical element can be used to convert the frequency of an electrical signal to a higher or lower frequency. This effect was used to modify the spectrum of oscillation of the current of an IREB.

The experimental arrangement is shown in Fig. 3. In the experiment an  $\sim 290$ -MHz sinusoidally bunched IREB<sup>11</sup> traversed a gap feeding a coaxial cavity with a resonance frequency of 3 times the 290 MHz, i.e., 870 MHz. The electron beam was confined by a 10-kG magnetic field and the base pressure inside the drift space was kept below  $\sim 5 \times 10^{-4}$  Torr. The input and output currents were measured at several places and are shown in Fig. 4 with the spectrum of  $dI/dt$ . Also in Fig. 4, we show an electrostatic probe signal displaying  $dE/dt$  at the gap where  $E$  is the electric field.

All cables, probes, attenuators, amplifiers, etc. were calibrated up to a frequency of 1 GHz. The output sig-

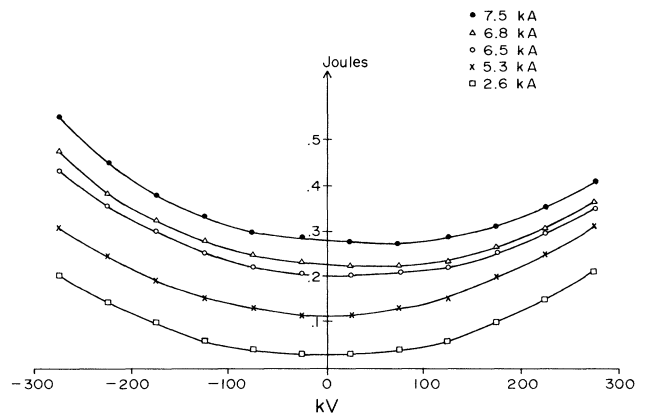


FIG. 2. The potential energy stored in the geometry of Fig. 1 (top) as a function of the applied voltage and of the propagating IREB current.

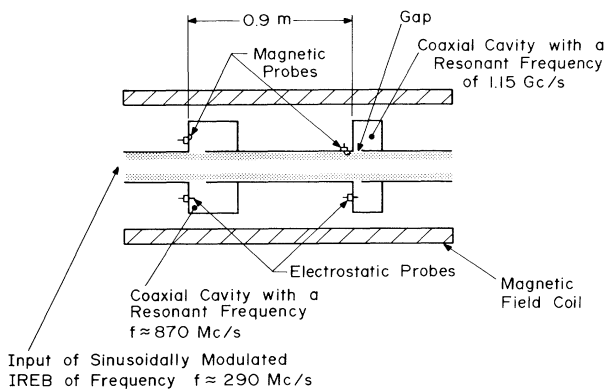


FIG. 3. Experimental configuration.

nals were corrected accordingly.

The nonlinear behavior of the gap can be seen when one compares the spectrum of  $dI/dt$  from the magnetic probe with the spectrum of  $dE/dt$  from the electrostatic probe, both located at the gap of the cavity [Figs. 4(a) and 4(b)]. While the current does not show any of the third harmonic and very little of second harmonic, the electrostatic probe displays large amplitude oscillations at these frequencies. Only the downstream magnetic probes show an increase of current modulation at the second and third harmonics [Fig. 4(c)].

The theoretical model of a gap is shown in Fig. 5. According to this model a constant-current source is feeding the following electrical elements: (1) a cavity, (2) a nonlinear capacitor  $C_g$ , and (3) a shunt conductance  $G$ . The current feeding the gap is equal to the modulated IREB current

$$I = I_0 + I_1 \exp(j\omega t) + I_2 \exp(j2\omega t).$$

Since the current is the source that generates the voltage on the gap and since  $C_g$  and  $G$  are functions of the voltage and current one can write

$$V = \sum V_l \exp[j(l\omega t)], \quad C_g = \sum C_n \exp[j(n\omega t)], \quad G = \sum G_m \exp[j(m\omega t)]; \tag{7}$$

and from the circuit equation one gets

$$V_1 = (-j) \frac{I_1}{\omega C_0 - Y(\omega) - jG_0}, \quad V_2 = (-j) \frac{I_2 - j(2\omega c_1)V_1 + G_1 V_1}{2\omega C_0 - Y(2\omega) - jG_0},$$

$$V_3 = (-j) \frac{(-j)(3\omega C_1 V_2 + 3\omega C_2 V_1) + G_1 V_2 + G_2 V_1}{3\omega C_0 - Y(3\omega) - jG_0}, \tag{8}$$

where  $Y(n\omega)^{-1} = Z \tan(n\omega L/c)$  and where  $\omega = 2\pi f$ ,  $f$  is the frequency of the fundamental,  $L$  is the length of the cavity,  $Z$  is the characteristic impedance of the cavity, and  $n$  is the harmonic number.

One can use the signals of the magnetic and electrostatic probes located at the gap to calculate  $C_1$  and  $C_2$ . This can be done by measurement of  $C_0$  from the resonance curve of the free space cavity and by the assumption that  $G_n$  is small in comparison with  $n\omega C_n$ .  $C_0$  was measured and found to be  $C_0 \approx 0.8$  pF. From

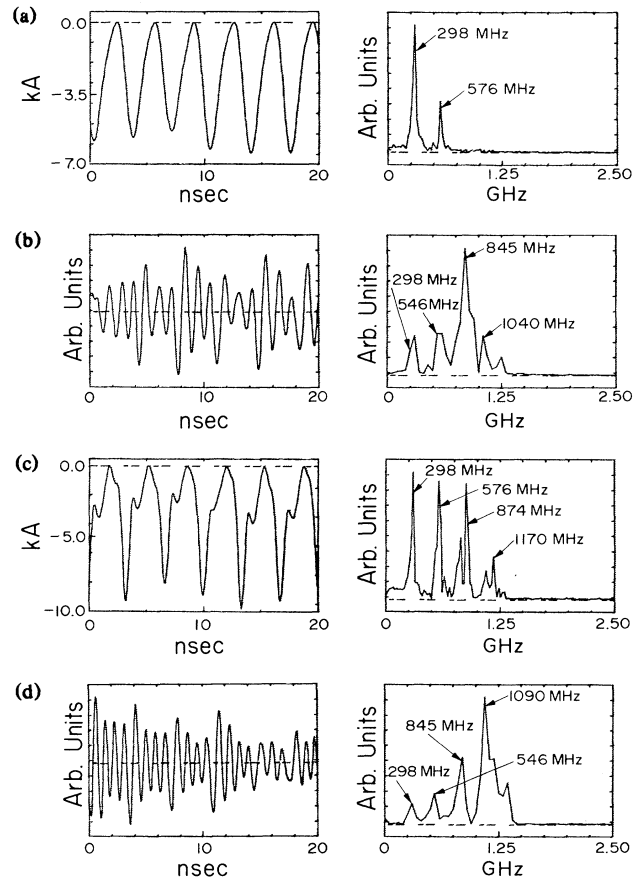


FIG. 4. (a) Current measured at the gap of the 870-MHz cavity and the spectrum of  $dI/dt$ . (b) Electrostatic signal measured at the gap of the 870-MHz cavity and its spectrum. (c) Current measured at 0.9 m downstream and the spectrum of  $dI/dt$ . (d) Electrostatic probe signal measured at the gap of the 1.15-GHz cavity and its spectrum.

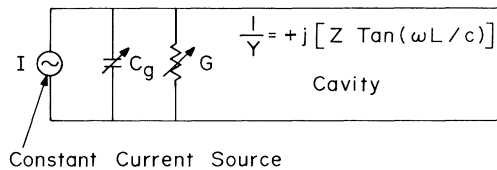


FIG. 5. The theoretical model that was used to explain the parametric interaction between an intense electron beam and a high-voltage gap.

Eq. (8) one calculates  $C_1 \approx 0.5$  pF and  $C_2 \approx 0.1$  pF. Although the electrostatic probe was calibrated only relatively one can calculate the voltage as a function of frequency at the gap using the values of  $C_0$ ,  $C_1$ ,  $C_2$ , the current at the gap, and Eq. (8):

$$V_1 \approx (1.5 \pm 0.1) \times 10^5 \text{ V},$$

$$V_2 \approx (1.0 \pm 0.3) \times 10^5 \text{ V},$$

$$V_3 \approx (3.0 \pm 1.0) \times 10^5 \text{ V}.$$

The voltage at the gap influences the current of the IREB. It was shown<sup>11</sup> that when an oscillating voltage,  $V^*$ , was applied at a gap located at an axial point  $z = 0$ , an oscillating current would be seen on the IREB at a point  $z$  downstream. For a large amplitude of  $V^*$ , current oscillations were found even at point  $z = 0$ . In the present experiment  $V^* = V_3$  is not large enough to generate  $I_3$  at the gap. However a large-amplitude current oscillation at the third harmonic was detected downstream of the gap. At the axial position where  $I_3$  reached its maximum, an additional coaxial cavity was inserted. The characteristic frequency of this cavity was tuned to the fourth harmonic ( $\approx 1.15$  GHz) of the initially sinusoidally modulated IREB. An electrostatic probe located at the gap of the additional cavity gave a signal containing a large amplitude of the fourth harmonic [Fig. 4(d)]. Theoretically, one can keep adding more cavities and get higher and higher harmonics.

Since it was possible to modulate IREB at frequencies of  $\sim 3$  GHz,<sup>14</sup> the above parametric affect will be

useful to generate a modulated IREB with a frequency spectrum that may extend beyond 10 GHz. The duration of each electron bunch in the modulated IREB will be  $\leq 0.1$  nsec with power in the  $10^{10}$ -W range. Such a beam will be useful for generation of microwaves and can also produce trains of subnanosecond-duration energetic x-ray pulses by electron bremsstrahlung.

<sup>1</sup>For example, see A. F. Harvey, *Microwave Engineering* (Academic, New York, 1963), Chap. 17.2.

<sup>2</sup>For example, see R. H. Freeman and A. E. Karboviak, *J. Phys. D* **10**, 633 (1977).

<sup>3</sup>J. R. Pierce, *J. Appl. Phys.* **30**, 1341 (1959).

<sup>4</sup>K. E. Lonngred *et al.*, *IEEE Trans. Plasma Phys.* **2**, 93 (1974).

<sup>5</sup>For example, see R. E. Collin, *Foundation for Microwave Engineering* (McGraw Hill, New York, 1966).

<sup>6</sup>H. Suhl, *Phys. Rev.* **106**, 384 (1957).

<sup>7</sup>T. J. Bridges, *Proc. IRE* **46**, 494 (1958).

<sup>8</sup>C. S. Bull, *Proc. Inst. Elect. Eng. Part B* **104**, 374 (1957).

<sup>9</sup>J. C. Martin, U.S. Patent No. 33 444 298 (1967).

<sup>10</sup>M. Friedman, *Appl. Phys. Lett.* **41**, 419 (1982).

<sup>11</sup>M. Friedman, V. Serlin, A. Drobot, and Larry Seftor, *Phys. Rev. Lett.* **50**, 1922 (1983), and *J. Appl. Phys.* **56**, 2459 (1984).

<sup>12</sup>M. Friedman and V. Serlin, *Appl. Phys. Lett.* **44**, 394 (1983).

<sup>13</sup>M. Friedman and V. Serlin, to be published.

<sup>14</sup>M. Friedman, *Appl. Phys. Lett.* **26**, 366 (1975).